Lawrence Berkeley National Laboratory
LBL Publications

Title
ACCELERATOR RESEARCH ON MBE-4 , AN EXPERIMENTAL MULTI-BEAM INDUCTION LINAC

Permalink
https://escholarship.org/uc/item/13b3q7rk

Authors
Meuth, H.
Fessenden, T.J.
Keefe, D.

Publication Date
1988-06-01

eScholarship.org Powered by the California Digital Library
University of California

UC-21
LBL-25098
c.1

Lawrence Berkeley Laboratory
UNIVERSITY OF CALIFORNIA

Accelerator & Fusion Research Division

RECEIVED
LAWRENCE
BERKELEY LABORATORY
DEC 21 1988
LIBRARY AND
DOCUMENTS SECTION

Presented at the International Symposium on
Heavy Ion Inertial Fusion, GSI, Darmstadt, FRG,
June 28–30, 1988

Accelerator Research on MBE-4, an Experimental Multi-beam Induction Linac

H. Meuth, T.J. Fessenden, D. Keefe, and A.I. Warwick

June 1988

For Reference

Not to be taken from this room

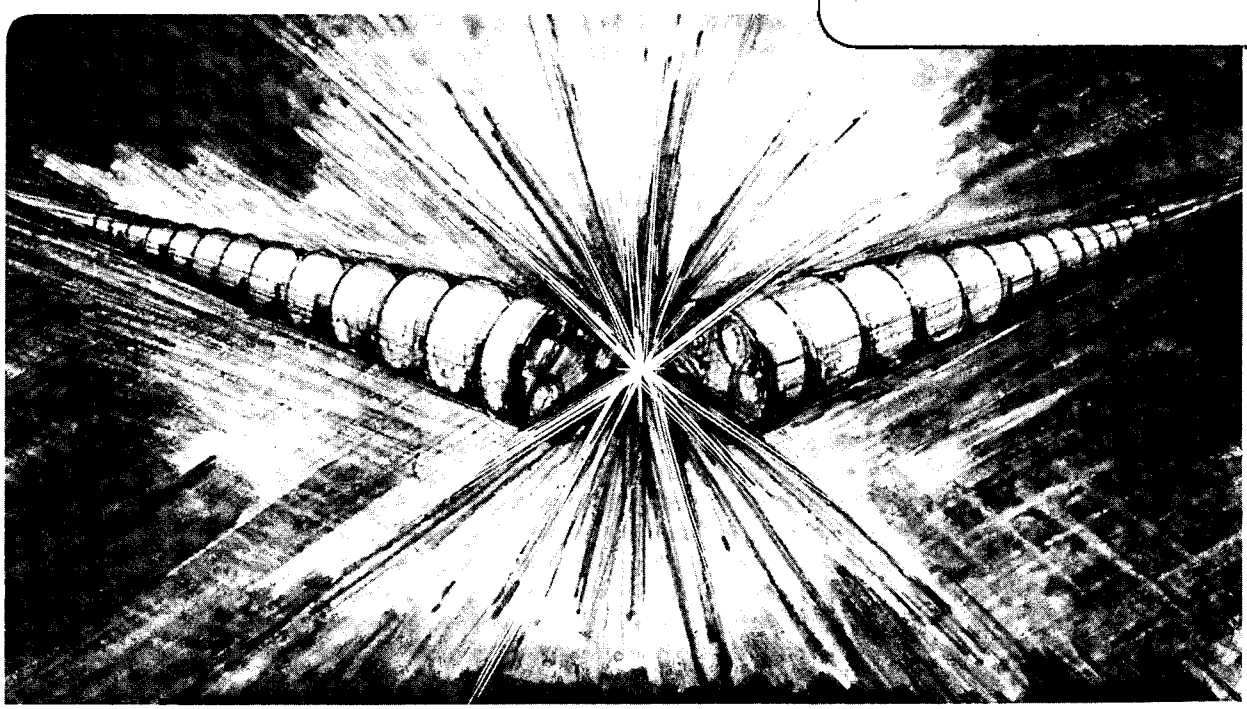

Prepared for the U.S. Department of Energy under Contract Number DE-AC03-76SF00098.

LBL-25098
c.1

DISCLAIMER

This document was prepared as an account of work sponsored by the United States Government. While this document is believed to contain correct information, neither the United States Government nor any agency thereof, nor the Regents of the University of California, nor any of their employees, makes any warranty, express or implied, or assumes any legal responsibility for the accuracy, completeness, or usefulness of any information, apparatus, product, or process disclosed, or represents that its use would not infringe privately owned rights. Reference herein to any specific commercial product, process, or service by its trade name, trademark, manufacturer, or otherwise, does not necessarily constitute or imply its endorsement, recommendation, or favoring by the United States Government or any agency thereof, or the Regents of the University of California. The views and opinions of authors expressed herein do not necessarily state or reflect those of the United States Government or any agency thereof or the Regents of the University of California.

LBL-25098
HIFAN-391

ACCELERATOR RESEARCH ON MBE-4, AN EXPERIMENTAL MULTI-BEAM INDUCTION LINAC*

H. Meuth, T.J. Fessenden, D. Keefe, and A.I. Warwick

Accelerator and Fusion Research Division
Lawrence Berkeley Laboratory
1 Cyclotron Road
Berkeley, California 94720
USA

June 1988

* This work was supported by the Office of Energy Research, Office of Basic Energy Sciences, U.S. Dept. of Energy under contract No. DE-AC03-76SF00098.

ACCELERATOR RESEARCH ON MBE-4, AN EXPERIMENTAL MULTI-BEAM INDUCTION LINAC *

H. Meuth, T.J. Fessenden, D. Keefe, and A.I. Warwick
Lawrence Berkeley Laboratory University of California Berkeley, CA . 94720, U.S.A.

Summary

The multiple beam accelerator MBE-4 is a device for research toward a heavy ion driver for inertial confinement fusion, based on the induction linac concept. Its main goal is proof of the principle of current amplification by acceleration and controlled self-similar beam pulse compression. Into the 16-m long device four beams, each with an initial current of 10 mA are injected from a Marx-driven diode at 200 keV. The current amplification is up to nine-fold, with a final beam energy of about 800 keV in the middle of the bunch. Now that all the apparatus' accelerator sections have been completed, installed and aligned, and its un-accelerated transport properties have been studied, our experimental research has reached the crucial phase of implementing appropriate accelerator schedules that approximate self-similar current-pulse compression. These schedules are established through a close interplay of computations using a one-dimensional simulation code and a manual empirical tuning procedure. In a first approach, with a rather vigorous schedule that uses most of the accelerator modules to their voltage limits, we have determined the limits of our capability for controlled pulse compression, mainly due to waveform shaping of the driving pulse-forming networks. We shall report on these results. In the future, we will also aim for gentler schedules that would model more closely an inertial confinement fusion scenario.

---

* This work was supported by the Office of Energy Research, Office of Basic Energy Sciences, U.S. Dept. of Energy under contract No. DE-AC03-76SF00098

Introduction

Two accelerator concepts are presently implemented to examine heavy-ion acceleration that might be suitable for inertial confinement fusion, namely the rf linac and storage ring system;[1] and the linear induction accelerator. The induction accelerator concept has been pursued for some time at the Lawrence Berkeley Laboratory, where a multiple-beam heavy ion linear accelerator, called MBE-4, has been recently completed.[2] This device is a scaled model experiment to study some of the issues that will arise in a heavy-ion driver for inertial confinement fusion. The four beams share the longitudinal acceleration gap structures and the corresponding driving modules, while being transversely contained in four separate focusing channels.

A four beam device was chosen to study the multiple-beam approach, which is needed in an HIF driver to reduce the required currents of several kiloamperes at the final focus to a technologically feasible level in each channel, especially in the early part of the accelerator, where the beam velocity is still low and space charge effects dominate. The transverse focusing in MBE-4 is electrostatic throughout its entire length. In a driver, the electrostatic focusing would be replaced by magnetic focusing in the later part of the accelerator, when increased ion velocities make this type of focusing more efficient.

Specific Features of MBE-4

Table I shows the salient physical and performance parameters of MBE-4. The schematic layout of MBE-4 is depicted in Fig. 1. In the matching section, the quadrupole doublets adapt the beams that emerge round from the thermonic diode[3] to the alternate gradient channels of the accelerator. Each gap between the quadrupoles in the matching section, and every fifth gap in the accelerator section serve for diagnostic access, while the accelerating voltages are applied to all the remaining gaps.

The design and performance features of the accelerator pulse-forming networks have been reported elsewhere.[4] Up to four pulsers per gap are available, whose amplitude and timing can each be programmed independently while their individual waveform patterns are essentially fixed by the specific choice of the circuitry components. The coupling cores, made from Nickel iron, and, for the modules with faster response time, from Silicon steel, constitute a non-linear load that modifies to some extent the waveform shape, depending on the amplitude setting.

Acceleration Schedules

The goal of the acceleration experiments is to show the feasibility of current amplification. The current $j=\lambda v$ may be increased (a) by accelerating the bulk of the ion bunch, thereby increasing the velocity v; and (b) by a differential head-to-tail acceleration for pulse compression, thereby increasing the line charge λ. In addition, to avoid bunch end erosion, very specific acceleration (or deceleration) is needed at the rise and fall of the current pulse. In the long-wavelength approximation, the longitudinal space charge electric fields are given by $E_z=-(g/4\pi\varepsilon_0\gamma^2)d\lambda/dz$ in terms of the line charge gradient and the usual relativistic coefficient γ. The empirical co-factor $g/4\pi\varepsilon_0$ models the electrostatic screening effects by the focusing channel. The force density λE_z is the essential ingredient for our one-dimensional code[5], that models the dynamics of a beam bunch made up from a small ($\leq$100) number of macro-particles during drift and/or acceleration through the device, using as initial conditions the measured current and energy pulse shape (see Fig. 2). This code served as an important design tool for the acceleration modules, and provides a guidance for establishing acceleration schedules (i.e. the setting of amplitude and timing of the individual modules), and, also, a diagnostic tool with the ongoing experiments to better understand the longitudinal beam dynamics in MBE-4, with and without acceleration. The parameter g (=2.2) was determined by fitting to the simulation the experimentally determined evolution (a) of a freely drifting beam bunch, and (b) of a drifting beam bunch that was "kicked" with an acceleration pulse at its midpoint.

Figure 3 shows the accelerating waveforms for the two types of pulsers used in MBE-4.[4] In figure 3a, the desired waveform, calculated by the simulation, is compared with the actually implemented waveform that was built up from three independent Thyratron pulsers at gap 4 (c.f. Fig. 1). At this gap, attempts were made to correct for the transient effects of the injector that show up in the beam kinetic energy at the bunch head and tail (c.f. Fig. 2). This correction appears not yet quite adequate, as can be seen from Fig. 3a. In sections D, E and F (c.f. Fig. 1), the bulk acceleration is achieved by spark-gap pulsers that produce a roughly square wave form across the induction cores. In Figure 3b, this is again compared with a desirable (or "ideal") waveform as computed by the simulation. Clearly, by this point higher frequency errors have accumulated.

Figure 4 shows the current pulses of the four beams at injection into the accelerator, and at the end, after acceleration. We observe that all beams are essentially equivalent, before and after acceleration. The corresponding current amplitudes and pulse widths are given in table I.

Longitudinal Dynamics

The measured current waveforms at all the diagnostic stations are shown in Fig. 5. The simulation tracks these measurements rather well throughout the major part of the accelerator (Fig. 6). However, in the last two sections the accumulation of slight voltage calibration and timing errors, as well as of errors emerging from the simulation, make such a comparison difficult, since the one-dimensional code cannot model correctly any possible particle overtaking. The indication of such an overtaking in the code may or may not be real and usually occurs at the head and tail of the bunch, where the actual acceleration waveforms match least the ideal ones that would be required for maintaining the bunch ends. These errors in the waveforms can also drive longitudinal space charge waves.[6] This suggests an early error correction, before kinetic particle energy has been converted into (electrostatic) potential energy.

The pulse compression requires a head-to-tail velocity tilt $\Delta\beta/\beta$. This tilt increases through the midpoint of MBE-4 . Thereafter, it decreases continuously but leads to further current amplification. Figure 7 shows $\Delta\beta/\beta$ and the kinetic energy at the head, center and tail of the bunch, along the accelerator, as they result from the simulation, and also the respective values at the end of the accelerator, as measured with an electrostatic energy analyzer. From this measurement, shown in Fig. 8, we can deduce a longitudinal emittance by estimating the area of the ellipse that encloses the particle distribution in longitudinal phase space

$$\varepsilon_z \sim 4 \times \pi \times 10^{-3}\text{eVs} \sim 10^{-2}\text{eVs}$$

The control of the distribution at the head is still inadequate, since it is perturbed by the leading edge of the accelerator waveforms that presently have too long a rise time (c.f. Fig. 3a).

Transverse Dynamics

The transverse dynamics, with and without acceleration, are determined with double slit scanners, inserted at various (axial) positions into the accelerator, and along both (transverse) principal axes. This diagnostic supplies the transverse beam distribution in (x, x')-phase space during the entire duration of the current pulse. From it we extract the temporal evolution of the rms-emittance, of the line-integrated transverse beam profile, and of the corresponding current bunch center by means of data evaluation routines that reside

on a PC-level computer that is also used for control of the experiment.[7] We will first discuss the emittance measurements.

Via a multi-shot scanning procedure, the double slit method records the cup signal vs. time, S(x,x',t) for the (x,x')-phase space area that is occupied by the beam. In Figure 9, the length of the bars represents this signal strength. The transverse bell-shaped distribution is clearly visible. But aside from the charge collection from the cup, the signal contains also a contribution from noise pick-up. This noise is particularly difficult to eliminate, when all acceleration modules are in operation, and is dominant wherever the beam signal amplitude is small. From the measurement S(x,x',t) the rms emittance ε_{rms} is calculated in the following fashion:

$$\varepsilon_{rms}^2 = \langle (x - \langle x \rangle_c)^2 \rangle_c \langle (x' - \langle x' \rangle_c)^2 \rangle_c - \langle (x - \langle x \rangle_c)(x' - \langle x' \rangle_c) \rangle_c^2 ,$$

where the (truncated) average of a function f(x,x',t) is derived from S by:

$$\langle f \rangle_c = \sum_{ij} f(x_i,x_j',t)\, S(x_i,x_j',t)\, \Theta(S(x_i,x_j',t)-c) \,/\, \sum_{ij} S(x_i,x_j',t)\, \Theta(S(x_i,x_j',t)-c) .$$

Here, c is the cut-off level of the signal, with $S_{min} \le c \le S_{max}$; for $S < c$, the distribution is truncated, signified here by the Heavyside function Θ. Correspondingly, we many define the percentage, P, of the total current that is thus included:

$$P = \sum_{ij} S(x_i,x_j',t)\, \Theta(S(x_i,x_j',t)-c) \,/\, \sum_{ij} S(x_i,x_j',t) .$$

The rms emittance is hence an implicit function of P via the cut-off level c. Plotting ε_{rms} vs. P (Fig. 9) we note three regimes with distinctly different slope (see also Fig. 10). With increasing cut-off level (or decreasing percentage of current), the first is governed by the noise contribution to the wings of the distribution, then the second by the halo and the third by the core of the beam . We discuss this point in some detail to show the importance of how to define the conditions under which the emittance values are quoted. The otherwise commonly used "95%"-value appears not suitable for MBE-4, since at this level the emittance is still largely determined by the electrical noise. Rather than giving here the emittance for a certain percentage value, we , therefore, present instead the detailed emittance-versus-cutoff plots for three locations (accelerator entrance, midpoint and exit), for both principal transverse axes (horizontal and vertical). Results for the unaccelerated and accelerated beams are compared. The normalized transverse emittance is thus of the

order of $4\pi\beta\gamma\varepsilon_{rms} \leq 0.15\ \pi \times 10^{-6}$ rad×m for the unaccelerated beam and appears to increase by a factor of two for the beam accelerated to four-fold energy. However, these data are still preliminary that will require confirmation. In any case, the mechanisms for emittance growth, if any, in MBE-4 are not understood at this point .

A second feature of the transverse dynamics are the coherent betatron oscillations that are driven by the large velocity tilt necessitated for pulse compression and transverse machine misalignments. In MBE-4, the transverse alternate gradient focusing system operates with dc-voltages. Consequently, due to head-to-tail tilt there will be necessarily some mismatch occurring during the pulse, leading to transverse oscillations in the bunch. Secondly, oscillations are induced due to transverse misalignments in the quadrupole focusing channels. After the mechanical completion of MBE-4 late 1987, the channels were aligned to within ± 0.13mm (rms). From estimates by Smith and Hahn[8] we expect oscillation amplitudes of a few millimeters, roughly in line with our measured results. Figure 11 shows these transverse oscillations of beam position and angle at the midpoint of the accelerator, where the velocity tilt has reached its maximum value (Fig. 7).

Future Outlook

With these first experimental results from the now completed MBE-4 accelerator device, we could pinpoint several issues that will have to be addressed in the future:

(a) the longitudinal pulse shape control has to be improved, particularly at head and tail. Limitations in hardware have to be evaluated regarding their effect in driving longitudinal current fluctuations.

(b) the (transverse) coherent betatron oscillation may make necessary steering of the beam to avoid the proximity to the focusing elements.

(c) transverse emittance measurements will have to be continued and the corresponding diagnostic techniques be refined to assert any possible emittance growth.

References

[1] See contributions to this conference by R. Bock; and by I. Hofman.

[2] T.J. Fessenden, D. Keefe, C H. Kim, H. Meuth, and A.I.Warwick: "The LBL Multiple Beam Experiments", Proc. IEEE Particle Accelerator Conference, Washington, D.C., March 1987, p. 898; T.J. Fessenden, D.L. Judd, D. Keefe, C.H. Kim, L.J. Laslett, L. Smith, and A.I. Warwick: "Preliminary Results from MBE-4: A Four-Beam Induction Linac for Heavy Ion Fusion Research", Proc. Int. Symposium on Heavy Ion Fusion, Washington, D.C., AIP conf. proc. 152, p. 145; R.T. Avery, C.S. Chavis, T.J. Fessenden, D.E. Gough , T.F. Henderson, D. Keefe, J.R. Meneghetti, C.D. Pike, D.L. Vanecek, and A.I. Warwick: "MBE-4, Heavy Ion Multiple Beam Experiment", Proc. IEEE Particle Accelerator Conference, Vancouver, B.C., May 1985, p. 3287.

[3] A.I. Warwick : "Alumino-Silicate Ion Sources for Accelerator Applications", ibid., p. 1809 ; A.I. Warwick., D. Vanecek, O Fredriksson: "A Four-Beam Cesium Injector for MBE-4", ibid., p. 3196.

[4] D. Gough, D. Brodzik, A. Faltens, C. Pike, and J. Stoker: "Pulsers for the Inducton Linac Experiment MBE-4", Proc. IEEE Particle Accelerator Conf., Washington D.C., March 1987, p. 954.

[5] C.H. Kim: "Ion Induction Linac Design and Operation Codes INDEX/SLID Users Manual", LBL, 1987 (unpublished); C.H. Kim and L. Smith: "Design Procedure for Acceleration and Bunching in an Ion Induction Linac", Particle Accelerators 18, 101 (1985).

[6] A.I. Warwick, T.J. Fessenden, D. Keefe, C.H. Kim, and H. Meuth: "Performance of MBE-4, an Experimental Multi Beam Induction Linear Accelerator for Heavy Ions", European Particle Accelerator Conference , Rome, June 1988.

[7] S.H. McCreight: "Instructions for MBE-4 Systems Programs", LBL, (unpublished).

[8] L. Smith and K.D. Hahn: "Transverse Mis-Alignments in a Driver", contribution to this conference.

Table I

type of ions	Cs^+		
	initial	final	
kinetic energy	200KeV	≤900KeV	@ center of bunch
ion velocity	5.7×10^5m/s	≤1.2×10^6m/s	@ center of bunch
beam current	4×10mA	4×85mA	@ center of bunch
line charge density	$4\times1.8\times10^{-8}$C/m	$4\times7\times10^{-8}$C/m	@ center of bunch
pulse duration	3μs	350ns	(FWHM)
bunch length	1.7m	0.45m	(FWHM)
total length of accelerator	14m		
tune depression	$\sigma_o=60^\circ$, $\sigma=12^\circ$		

Figure Captions

Fig. 1: Schematic layout of the accelerator.

Fig. 2: Current and energy of beam pulse at injection.

Fig. 3: Ideal (---) and actual (···) accelerating waveforms from (a) Thyratron pulsers (box 4), and (b) spark-gap pulsers (box 17).

Fig. 4: Current pulse waveforms (a) before (box M4), and (b) after (box 30) acceleration.

Fig. 5: Current pulse waveforms at all diagnostic stations of accelerator.

Fig. 6: Comparison of simulation and measurements.

Fig. 7: Velocity tilt and kinetic beam energy along accelerator.

Fig. 8: Kinetic energy measurement at box 30.

Fig. 9: Emittance versus percent of beam current.

Fig. 10: Emittance measurements at entrance (box M4), midpoint (box 15), and exit (box 30) of accelerator.

Fig. 11: Transverse oscillations in beam bunch (box 15).

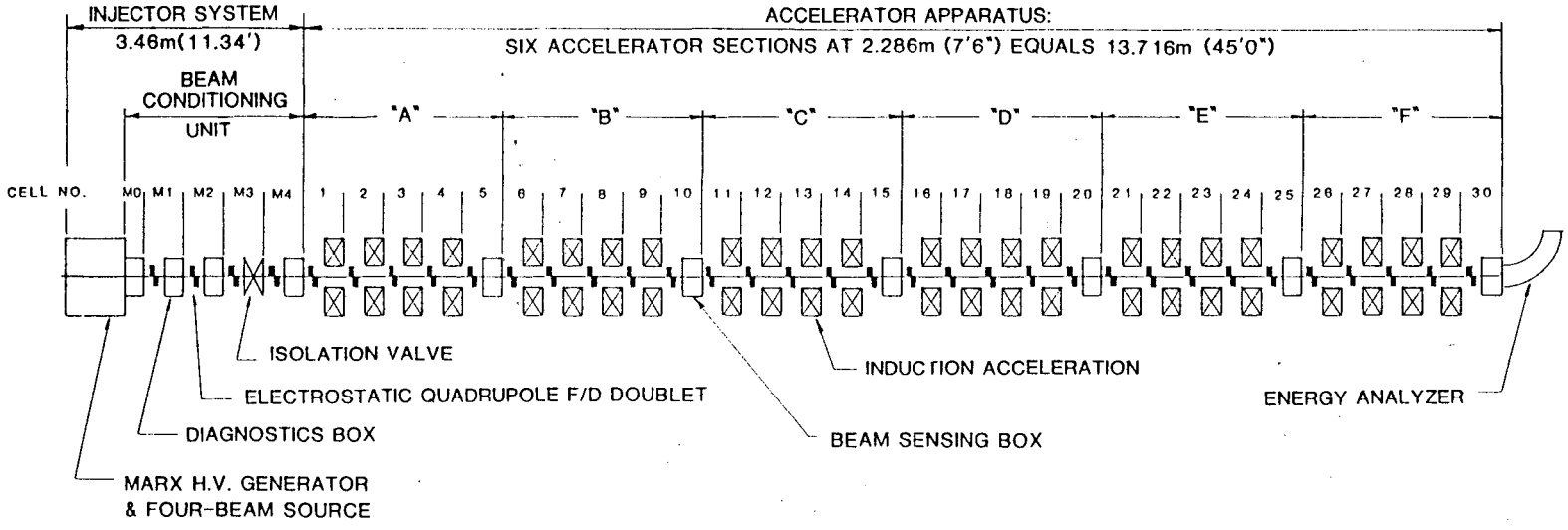

MBE-4
DIAGRAMMATIC LAYOUT

XBL 854-2077

Fig. 1

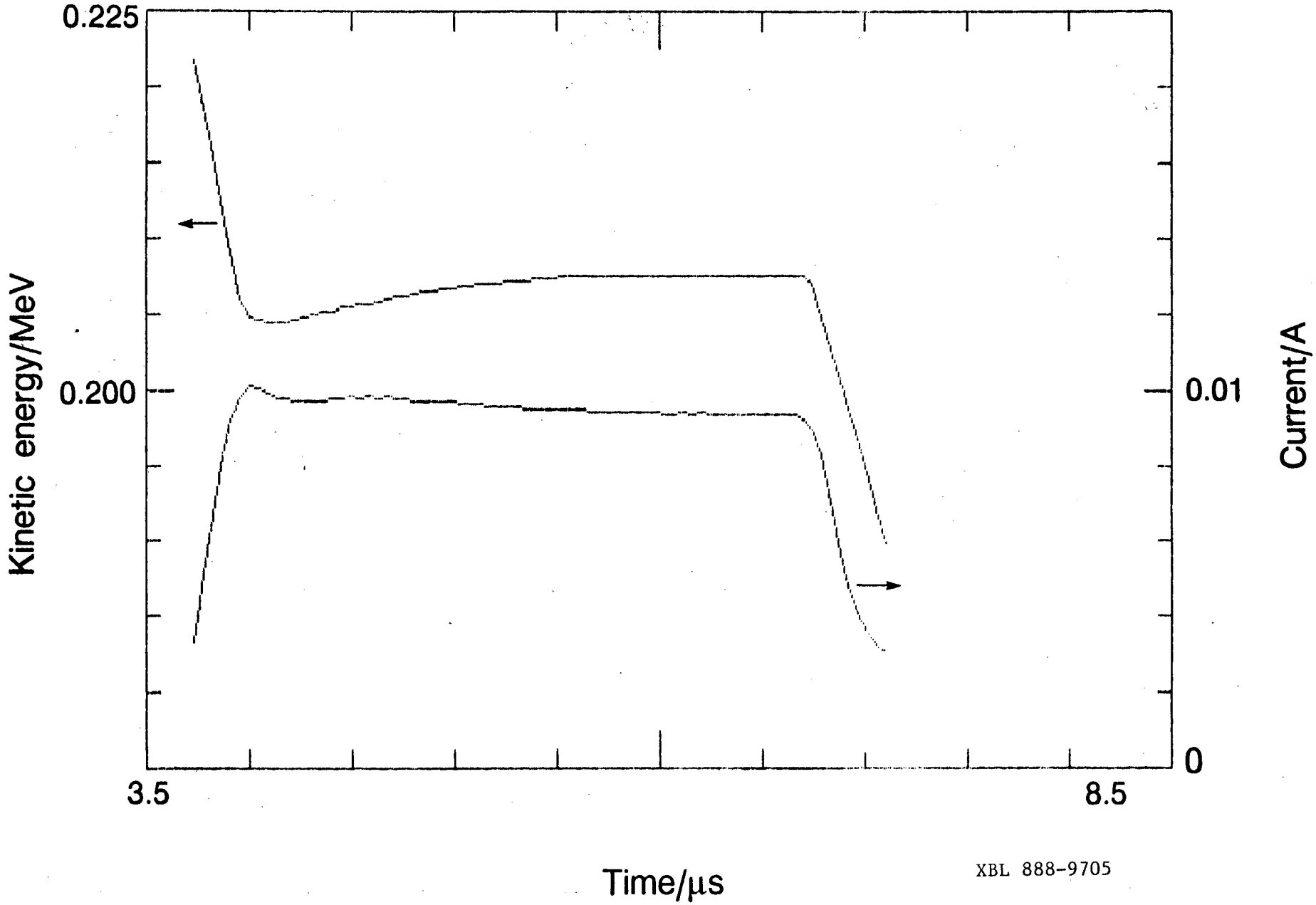
0.225
0.200
Kinetic energy/MeV
0.01
0
Current/A
3.5
8.5
Time/μs
XBL 888-9705

Fig. 2

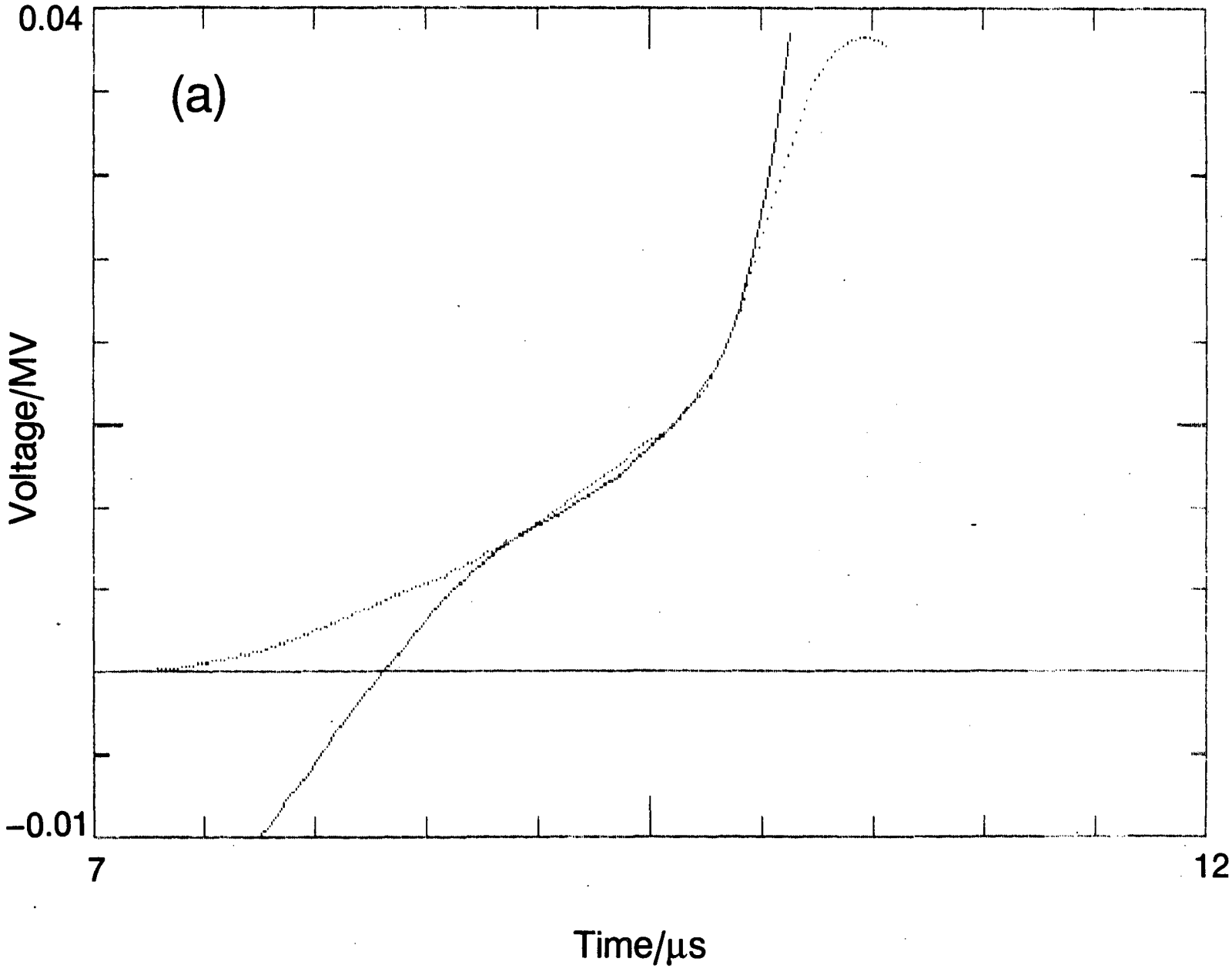

Fig. 3a

XBL 888-9707

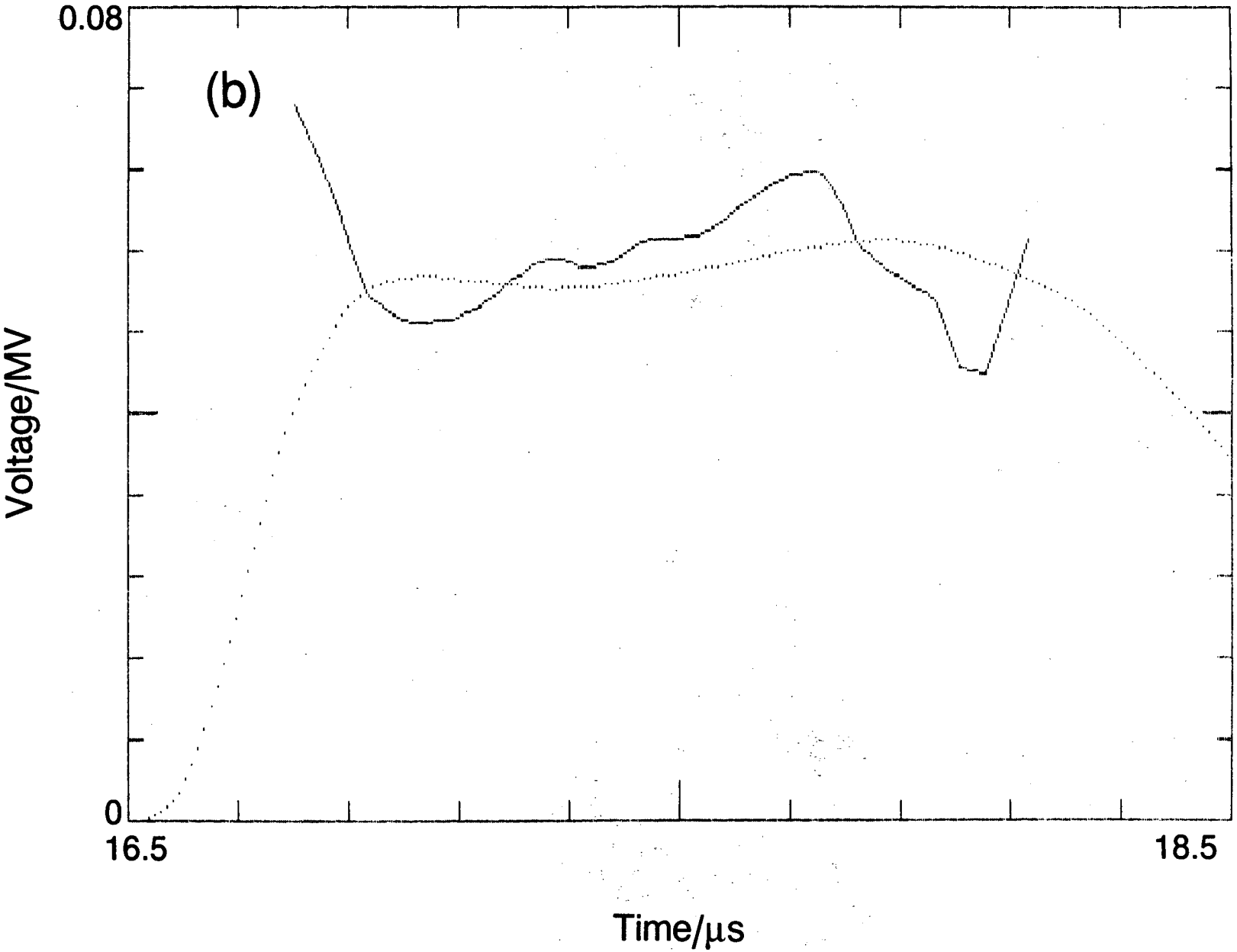

Fig. 3b

XBL 888-9704

Fig. 4a

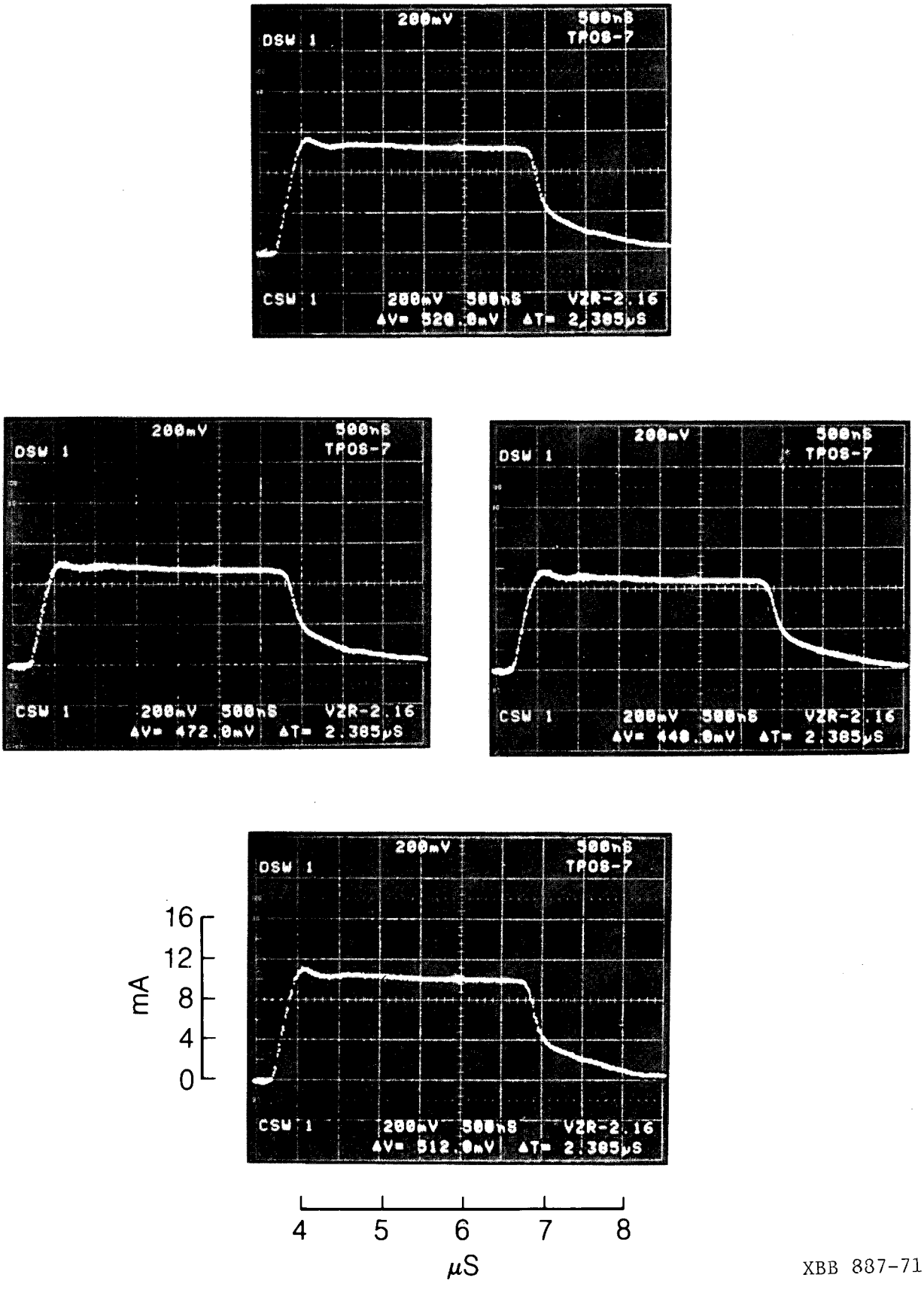

XBB 887-7122

Fig. 4b

Top

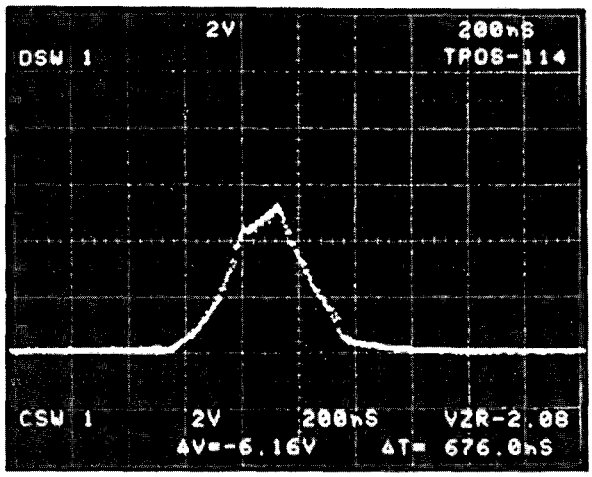

Left

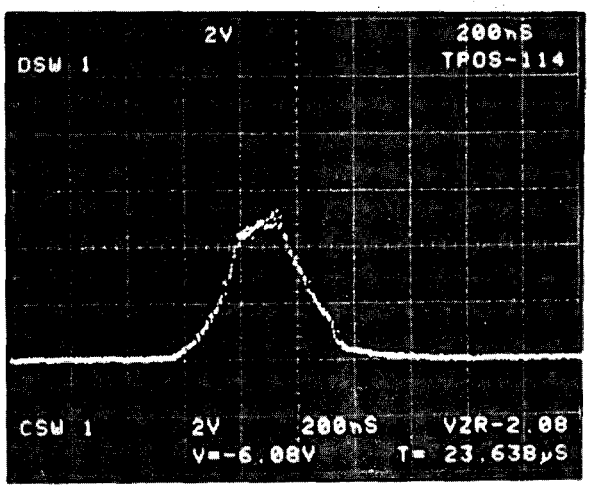

Right

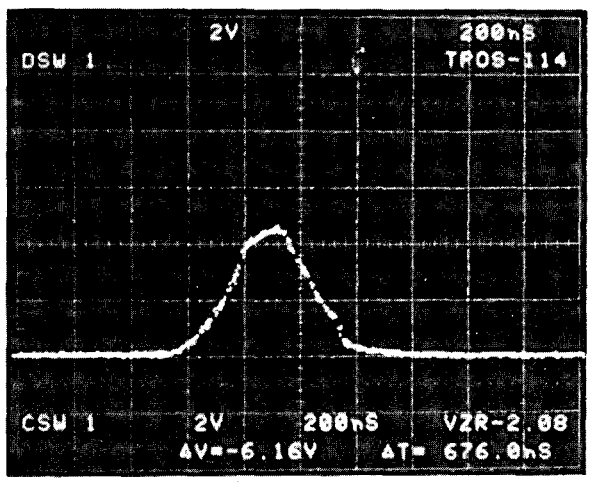

Bottom

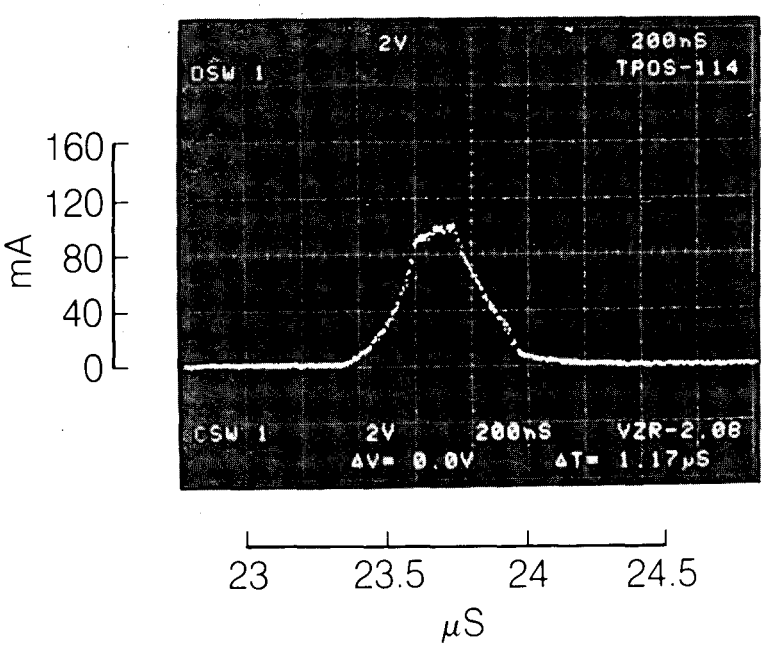

XBB 880-9450

Fig. 5

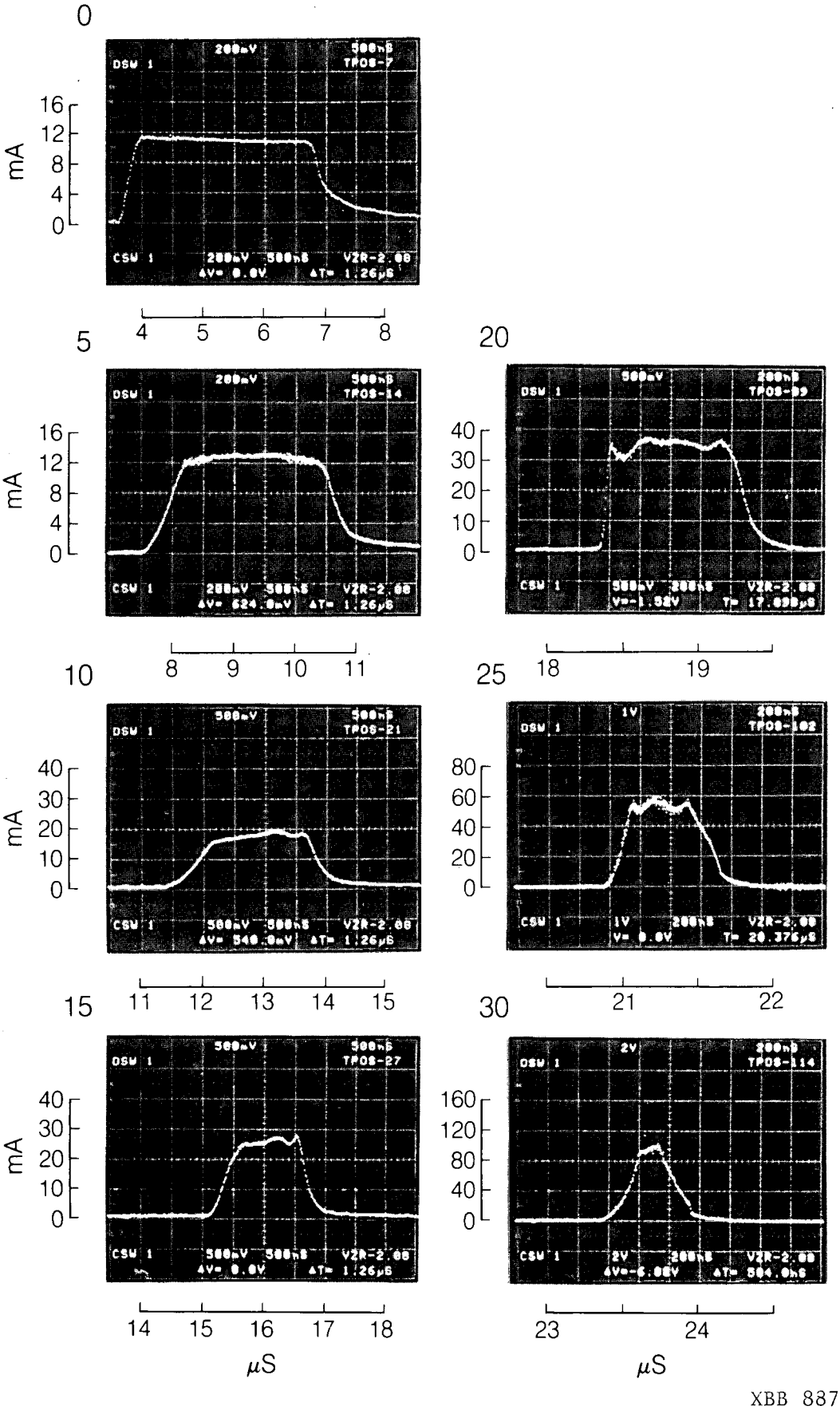

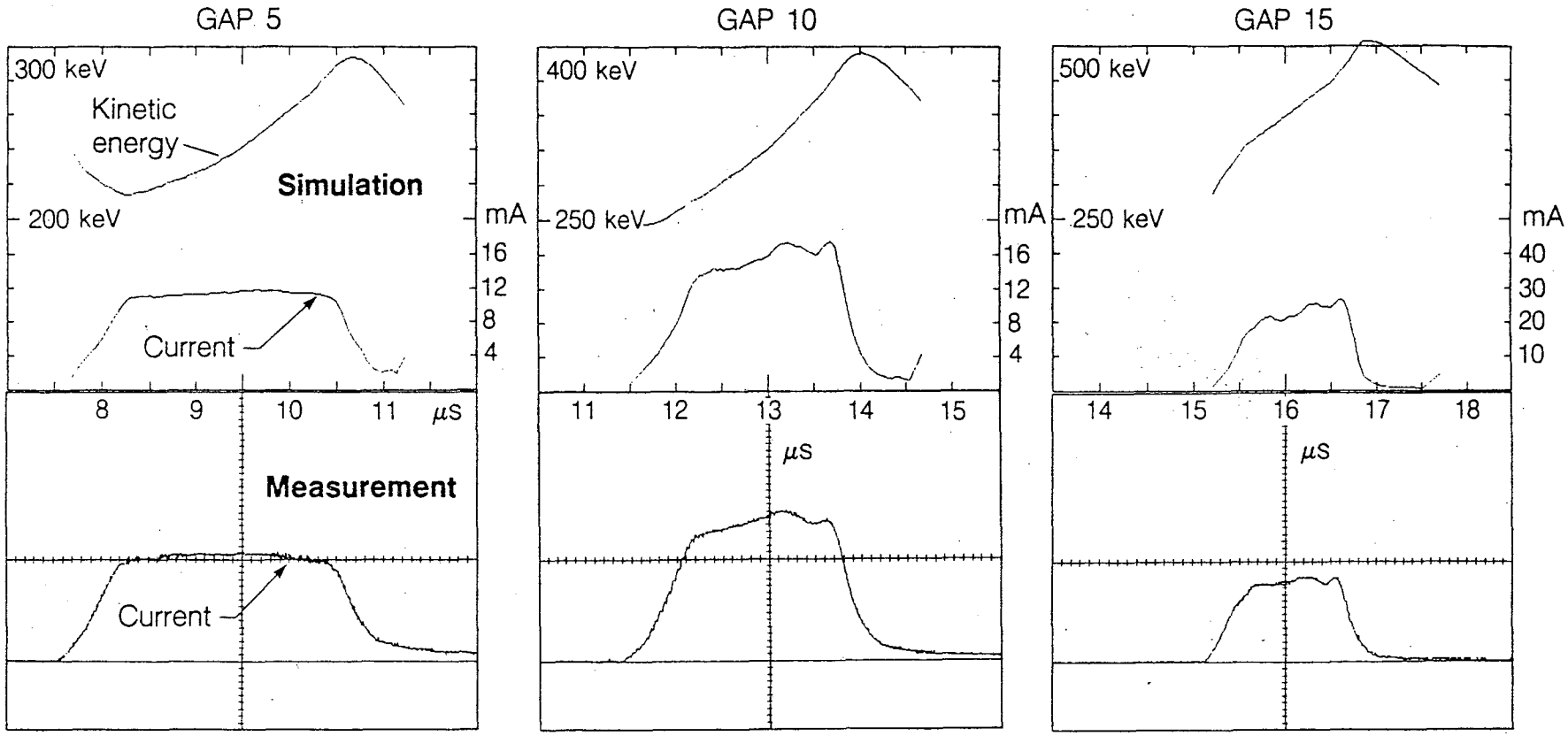

XBL 885-8892

Fig. 6

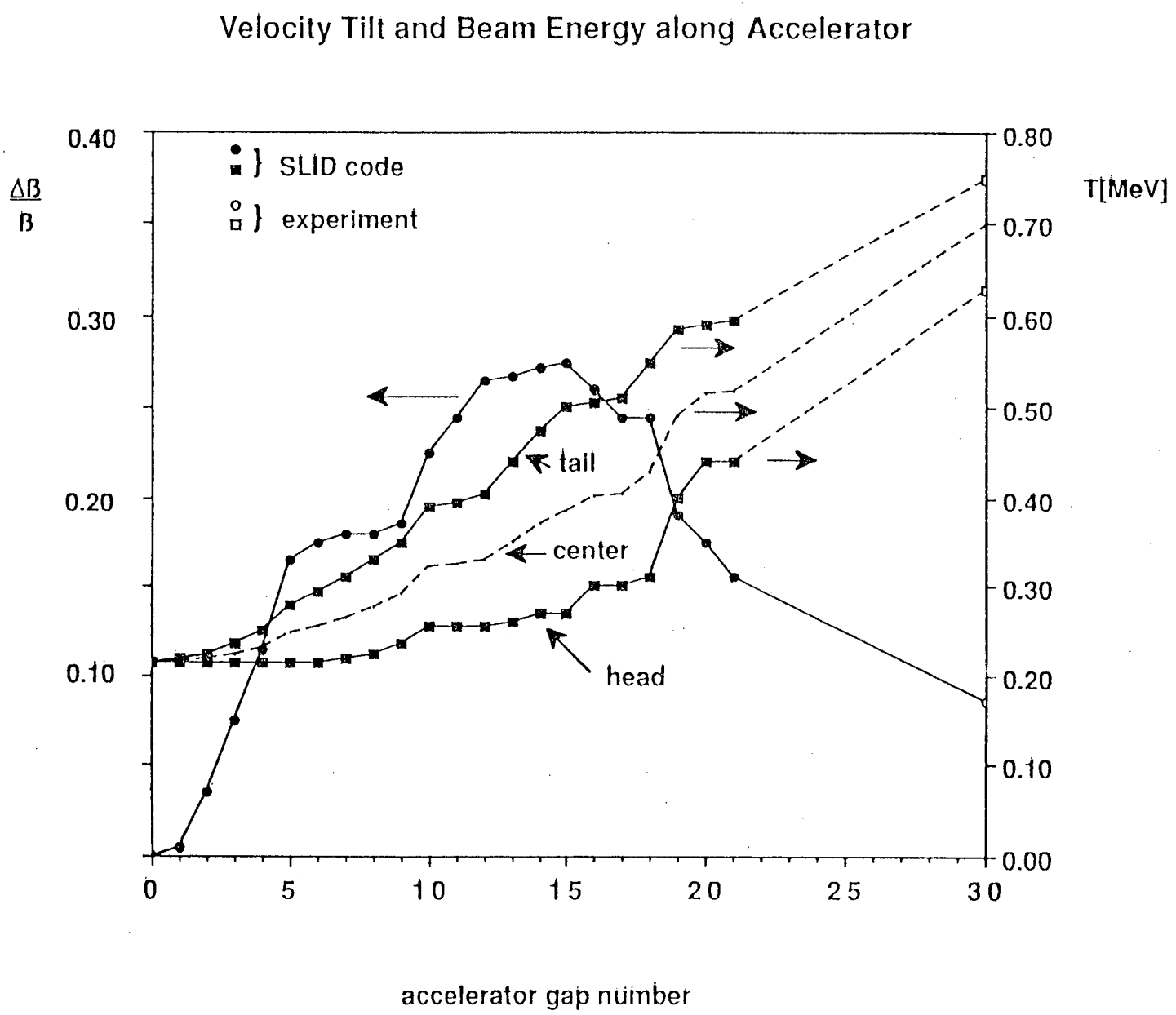
Velocity Tilt and Beam Energy along Accelerator
0.40
0.30
0.20
0.10
ΔB/B
SLID code
experiment
tail
center
head
0.80
0.70
0.60
0.50
0.40
0.30
0.20
0.10
0.00
T[MeV]
0
5
10
15
20
25
30
accelerator gap number

Fig. 7

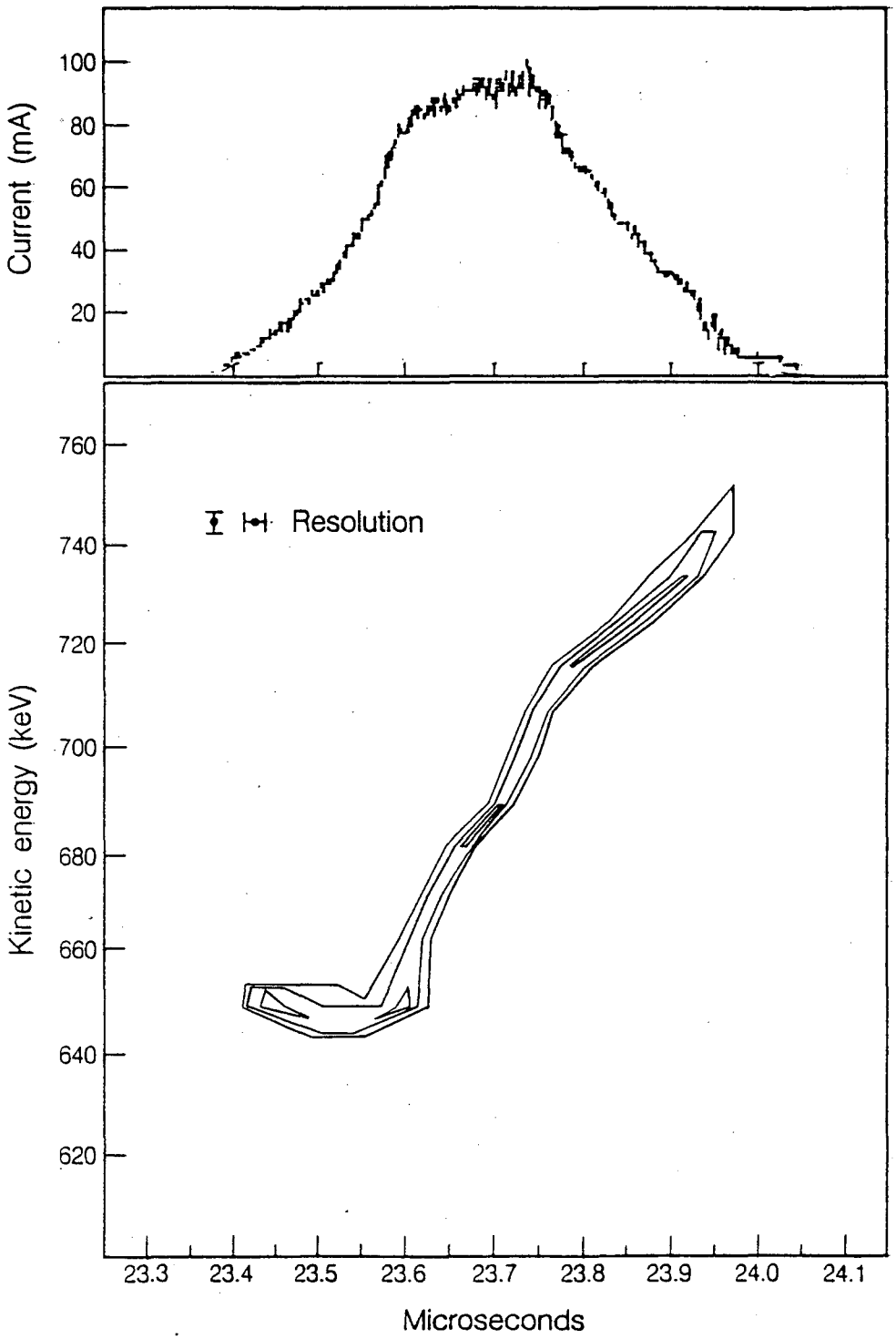

XBL 885-8891

Fig. 8

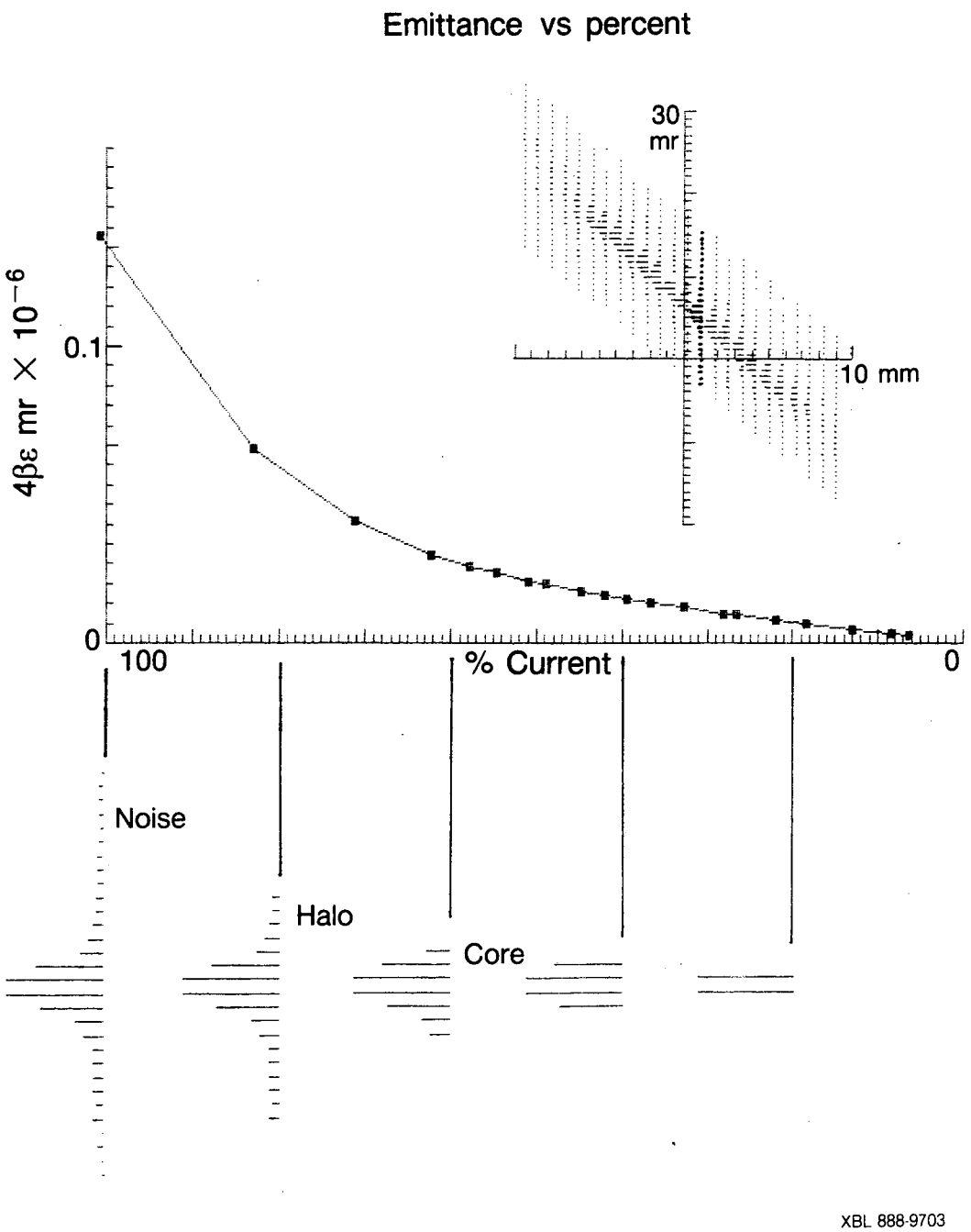
Emittance vs percent
30
mr
10 mm
$4\beta\varepsilon$ mr $\times 10^{-6}$
0.1
0
100
% Current
0
Noise
Halo
Core
XBL 888-9703

Fig. 9

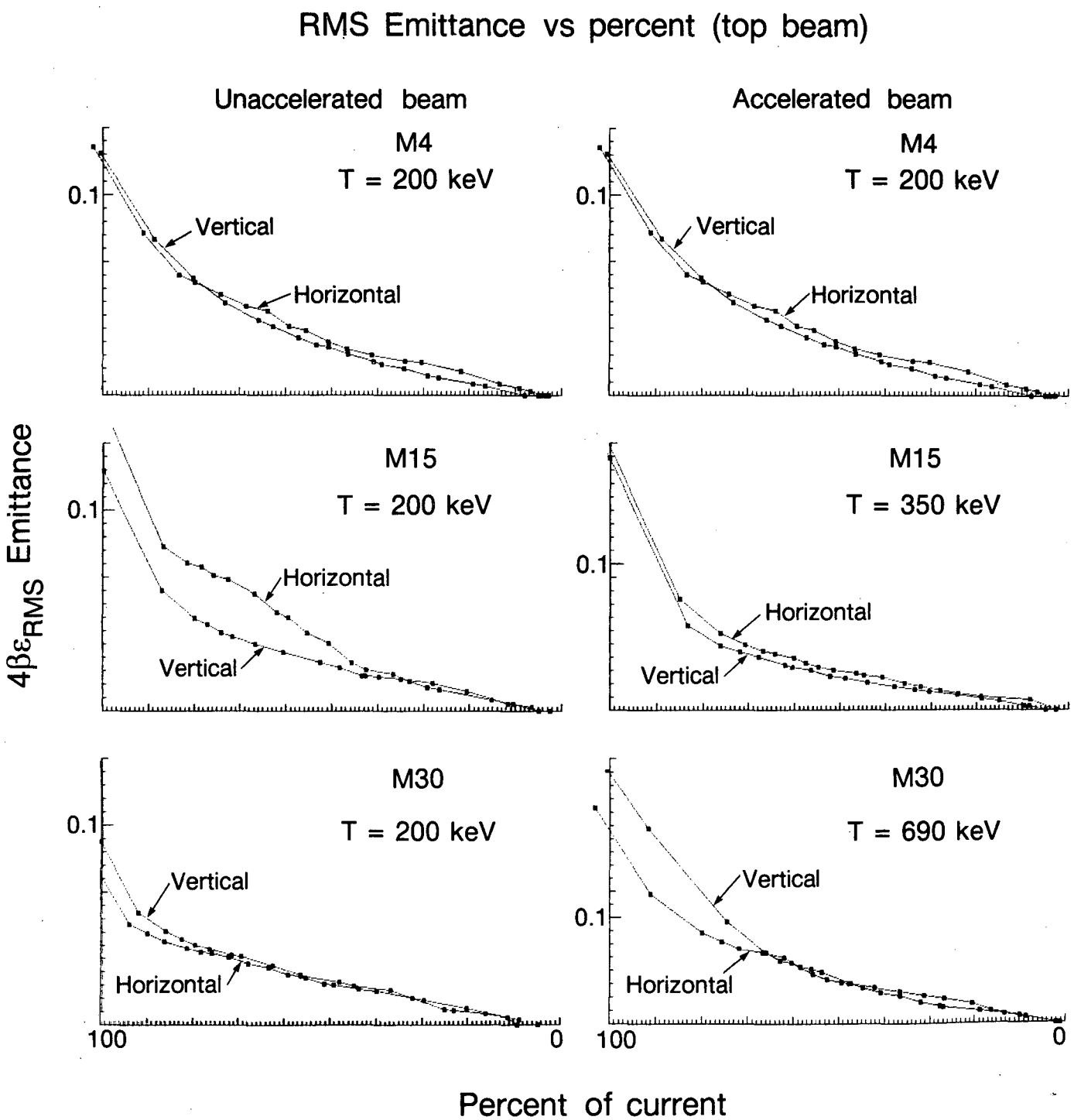
RMS Emittance vs percent (top beam)
Unaccelerated beam
Accelerated beam
M4
T = 200 keV
Vertical
Horizontal
M15
T = 200 keV
M15
T = 350 keV
M30
T = 200 keV
M30
T = 690 keV
0.1
$4\beta\varepsilon_{RMS}$ Emittance
100
0
Percent of current
XBL 888-9706

Fig. 10

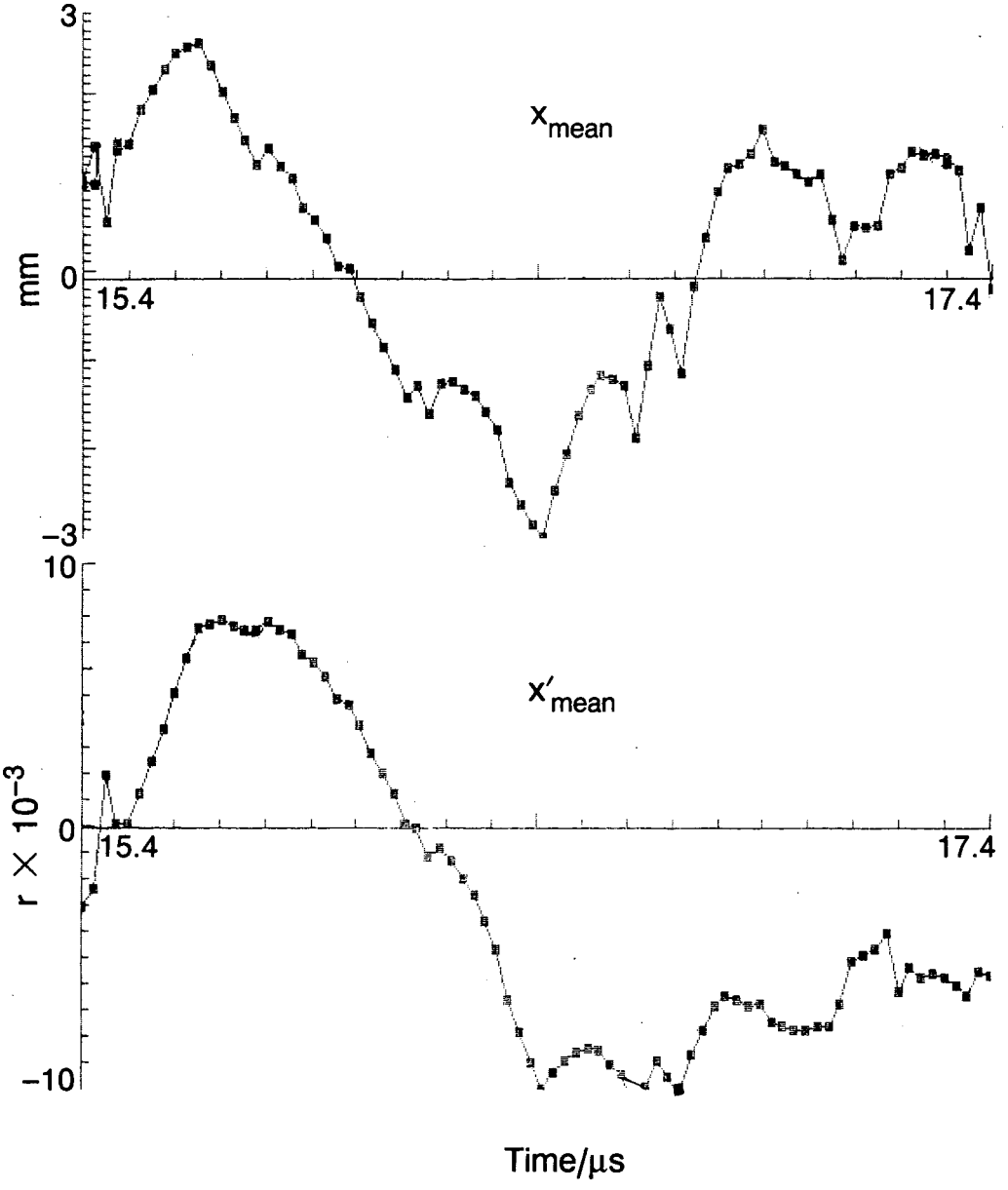
3
0
−3
mm
x_{mean}
15.4
17.4
10
0
−10
r × 10⁻³
x'_{mean}
15.4
17.4
Time/μs
XBL 888-9702

Fig. 11

LAWRENCE BERKELEY LABORATORY
TECHNICAL INFORMATION DEPARTMENT
1 CYCLOTRON ROAD
BERKELEY, CALIFORNIA 94720